lection. Intensity measurements were made on a Nicolet R3m/V diffractometer using graphite-monochromated Mo Kα radiation with 3.5° < 2θ < 50°, operating in an ω-scan mode with a scan range of 1.20°, at a scan rate between 3.00 and 15.00° min^{-1}. A total of 5091 unique data were collected ($\pm h,+k,+l$), 3151 of which were considered to be observed [$F \geq 6\sigma(F)$]. Three standard reflections monitored every 197 reflections showed no significant variation in intensity over the data collection period. No absorption correction was applied because the faces of the crystal were poorly defined and difficult to identify. Intensity data were corrected for Lorentz and polarization effects. The atomic scattering factors for neutral atoms were taken from ref 28 and were corrected for anomalous dispersion. All calculations were performed on a MicroVAX 2000 computer. The program used for least-squares refinement was that due to Sheldrick.[29]

The structure was solved by Patterson methods. Full-matrix least-squares refinement employing anisotropic thermal parameters for all non-hydrogen atoms and a single-variable isotropic thermal parameter for hydrogen that refined to 0.17 (1) Å^2, located in geometrically idealized positions (C-H = 0.96 Å), reduced R to 0.048 and R_w to 0.046, respectively, at convergence, where $R_w = (\sum w(|F_o| - |F_c|)^2/\sum w(|F_o|^2)^{1/2}$ and $w = [\sigma^2(F_o)]^{-1}$ The goodness of fit value $([\sum w(|F_o| - |F_c|)^2/(N_{observns} - N_{params})]^{1/2}$ was 2.22. The largest peak in the *difference Fourier synthesis* was 0.80 e Å^{-3}.

Acknowledgment. This work was supported by a Monash Research Grant, the Australian Research Council, and Johnson-Matthey through a loan of rhodium trichloride.

Supplementary Material Available: Tables of all bond lengths (Table S1) and bond angles (Table S2), anisotropic displacement coefficients (Table S3), and hydrogen atom coordinates (Table S4) and a unit cell and crystal packing diagram of the Rh(III) dimer (Figure S1) (5 pages); a listing of observed and calculated structure factors (Table S5) (18 pages). Ordering information is given on any current masthead page.

(28) Ibers, J. A.; Hamilton, W. C., Eds. *International Tables for X-ray Crystallography*; Kynoch Press: Birmingham, England, 1974; Vol. IV.
(29) Sheldrick, G. M. *SHELXTL PLUS, Revision 3.4*; Siemens Analytical Instruments, Inc.: Madison, WI, 1988.

Contribution from the Department of Chemistry, University of Minnesota, Minneapolis, Minnesota 55455

Photochemical Generation of Reactive Transition-Metal Intermediates from Air-Stable Precursors. Carbon-Hydrogen Bond Activation via Near-Ultraviolet Photolysis of Cp*Ir(L)(oxalate) and Cp*Ir(L)$(N_3)_2$ Complexes

Daniel A. Freedman and Kent R. Mann*

Received June 15, 1990

We have synthesized several new oxalate and azide complexes of the form Cp*Ir(Ox)L (Cp* = pentamethylcyclopentadienyl, Ox = oxalate and L = $P(Me)_3$, $P(Cy)_3$) and Cp*Ir$(N_3)_2$L (L = $P(Me)_3$, $P(Ph)_3$, $P(Cy)_3$, and *t*-BuNC) respectively. Upon photolysis, these complexes undergo reactions that result in the elimination of CO_2 or N_2 to give reactive intermediates that undergo net oxidative-addition reactions with C-H and C-Cl bonds. We have observed either intermolecular (reaction with solvent) or intramolecular (reaction with a ligand bond) oxidative addition to the Ir center. For photolysis of the azide complexes in benzene solutions, the mode of reaction is determined by L. An exclusively intermolecular reaction is observed when L = $P(Me)_3$, while products indicative of inter- and intramolecular reactivity are observed with $P(Ph)_3$. The $P(Cy)_3$ complexes produce two different orthometalated complexes we identify as the cis and trans isomers, which arise from activation of either the axial or equatorial hydrogen on the α carbon of a cyclohexyl ring. Photolysis of the oxalate complexes in CCl_4, $CHCl_3$, or CH_2Cl_2 produces the corresponding dichloride. For the photolysis of Cp*Ir(Ox)$(P(Me)_3)$ in $CHCl_3$ and CH_2Cl_2, intermediates are observed. These intermediates result from the initial oxidative addition of C-Cl bonds of the solvent. The quantum yields for the oxalate photochemical reactions with halocarbons are in the range 0.02-0.28. For the azide complexes, the identity of L has little effect on the quantum yield. Similar quantum yields are observed for reaction in C_6H_6, $CHCl_3$, and CH_2Cl_2; substantially larger quantum yields are observed for CCl_4 solutions. In the case of the oxalate complexes, the quantum yield correlates inversely with the hydrogen-bonding ability of the solvent, resulting in the curious quantum yield ordering $CHCl_3 \approx CH_2Cl_2 < C_6H_6$. IR spectral data indicate significant shifts for the ν(CO) frequencies of the oxalate bands in solvents of even moderate H-bonding ability. We suggest that H-bonding enhances nonradiative excited-state decay, which controls the quantum yields of the oxalate complexes. The enhanced reactivity observed for the azide and oxalate complexes in CCl_4 is due to an electron-transfer mechanism from the photogenerated excited state to the solvent.

Introduction

Carbon-hydrogen bond activation has received a great deal of attention in recent years. Of particular interest are the photochemical systems developed by the Bergman[1-4] and Graham[5-7] groups:

$$Cp^*M(H)_2PR_3 \xrightarrow[R-H]{h\nu} Cp^*M(R)(H)PR_3 + H_2 \quad (1)$$

$$Cp^*M(CO)_2 \xrightarrow[R-H]{h\nu} Cp^*M(R)(H)CO + CO \quad (2)$$

M = Rh, Ir; Cp* = pentamethylcyclopentadienyl; PR_3 = trimethylphosphine; R-H = aromatic, aliphatic

Photochemical extrusion of CO or H_2 results in oxidative addition of C-H bonds. The proposed photogenerated intermediates in both of these systems react with a wide variety of substrates that include unactivated hydrocarbons (e.g. methane).[4,5] It is becoming increasingly clear as illustrated through studies of reaction 2 by several groups that photolysis of the bis(carbonyl) complex in inert-gas matrices or in liquified inert gases[8-10] results in the loss of CO in the primary photochemical reaction to form the coordinatively unsaturated CpM(CO) complex.[11] A similar, but even more reactive, intermediate is generated via reaction 1 from the

* To whom correspondence should be addressed.

(1) Janowicz, A. H.; Bergman, R. G. *J. Am. Chem. Soc.* **1982**, *104*, 352.
(2) Janowicz, A. H.; Bergman, R. G. *J. Am. Chem. Soc.* **1983**, *105*, 3929.
(3) Wax, M. J.; Stryker, J. M.; Buchanan, J. M., Kovak, C. A.; Bergman, R. G. *J. Am. Chem. Soc.* **1984**, *106*, 1121.
(4) Sponsler, M. B.; Weiller, B. H.; Stoutland, P. O.; Bergman, R. G. *J. Am. Chem. Soc.* **1989**, *111*, 6841.
(5) Hoyano, J. K. McMaster, A. D.; Graham, W. A. G. *J. Am. Chem. Soc.* **1983**, *105*, 7190.
(6) Ghosh, C. K.; Graham, W. A. G. *J. Am. Chem. Soc.* **1989**, *111*, 375.
(7) Hoyano, J. K.; Graham, W. A. G. *J. Am. Chem. Soc.* **1982**, *104*, 3723.
(8) Weiller, B. H.; Wasserman, E. P.; Bergman, R. G.; Moore, C. B.; Pimentel, G. C. *J. Am. Chem. Soc.* **1989**, *111*, 8288.
(9) Haddleton, D. H. *J. Organomet. Chem.* **1986**, *311*, C21.
(10) Graham, W. A. G. *J. Organomet. Chem.* **1986**, *300*, 81.
(11) Evidence suggests that in liquid xenon solutions the open coordination site is occupied by a solvent molecule.

0020-1669/91/1330-0836$02.50/0

photolysis of the air-sensitive dihydride complex. In this case, efficient activation of hydrocarbon bonds has been achieved.

Previous photochemical studies of azide and oxalate complexes[12-16] suggested to us that reactions 3 and 4 might offer more convenient chances to study the generation and subsequent reaction chemistry of intermediates analogous to those generated in reactions 1 and 2. We thought that these reactions might provide

$$Cp^*Ir(L)(N_3)_2 \xrightarrow{h\nu} Cp^*IrL + 3N_2 \quad (3)$$

$$Cp^*Ir(L)(Ox) \xrightarrow{h\nu} Cp^*IrL + 2CO_2 \quad (4)$$

$$Ox = \eta^2\text{oxalate}$$

access to highly reactive intermediates from easily synthesized, stable starting materials. Additionally, reactions such as (3) and (4) could be conveniently monitored by following the strong infrared spectral bands of the azide and oxalate functional groups. To this end, we have synthesized azide and oxalate complexes of the form indicated in eqs 3 and 4 and report on our initial photochemical studies. These studies suggest that, in several cases, highly reactive intermediates with reaction chemistry analogous to those produced in eqs 1 and 2 are formed.

Experimental Section

General Considerations. All synthetic procedures were carried out under an inert N_2 atmosphere. Solvents were of spectroscopic grade and were used without further purification unless otherwise noted. ^1H and ^{13}C NMR spectra were recorded on IBM AC-200 or AC-300 NMR spectrometers. Chemical shifts are recorded relative to $(CH_3)_4Si$. IR spectra were recorded on a Perkin-Elmer 1600 IR spectrometer. Elemental analyses were performed by MHW Laboratories. $[Cp^*IrCl_2]_2$[17] and $[Cp^*Ir(N_3)_2]_2$[18] were prepared via procedures reported for the synthesis of the rhodium analogues.

Compound Synthesis. $Cp^*Ir(N_3)_2P(Me)_3$. $P(Me)_3$ (0.05 mL, 0.483 mmol) was added to a solution of $[Cp^*Ir(N_3)_2]_2$ (100 mg, 0.122 mmol) in 15 mL of methylene chloride. The solution was stirred overnight under a flow of nitrogen to evaporate the solvent and excess $P(Me)_3$ to give a bright yellow powder. The product was dissolved in methylene chloride and precipitated with hexane to yield 0.1006 g (85% yield) of bright yellow microcrystals. Anal. Calcd for $C_{13}H_{24}IrN_6P$: C, 32.03; H, 4.96; N, 17.24. Found: C, 32.07; H, 5.11; N, 17.49. ^1H NMR (200 MHz, $CDCl_3$): δ 1.796 (d, C_5Me_5, 15 H, J_{P-H} = 2.18 Hz), 1.653 (d, $P(Me)_3$, 9 H, J_{P-H} = 11.0 Hz).

$Cp^*Ir(N_3)_2P(Ph)_3$. This compound was prepared in a manner analogous to that used for $Cp^*Ir(N_3)_2P(Me)_3$ with $P(Ph)_3$ substituted for $P(Me)_3$. The compound was isolated as bright yellow microcrystals in 80% yield. Anal. Calcd for $C_{28}H_{30}IrN_6P$: C, 49.91; H, 4.49; N, 12.47. Found: C, 49.74; H, 4.62; N, 12.28. ^1H NMR (200 MHz, CD_2Cl_2): δ 1.476 (d, C_5Me_5, 15 H, J_{P-H} = 2.4 Hz), 7.420–7.458 (m, $P(Ph)_3$, 15 H).

$Cp^*Ir(N_3)_2P(Cy)_3$. This compound was prepared in a manner analogous to that used for $Cp^*Ir(N_3)_2P(Me)_3$ with $P(Cy)_3$ substituted for $P(Me)_3$. The compound was isolated as bright orange flakes in 88% yield. Anal. Calcd for $C_{28}H_{48}IrN_6P$: C, 49.00; H, 7.01; N, 12.15. Found: C, 48.89; H, 6.87; N, 11.96. ^1H NMR (200 MHz, $CDCl_3$): δ 1.730 (d, C_5Me_5, 15 H, J_{P-H} = 1.6 Hz), 1.26–2.21 (m, $P(Cy)_3$, 33 H,).

$Cp^*Ir(N_3)_2(CN\text{-}t\text{-}Bu)$. This compound was prepared in a manner analogous to that used for $Cp^*Ir(N_3)_2P(Me)_3$ with *t*-BuNC substituted for $P(Me)_3$. The compound was isolated as bright yellow-orange microcrystals in 72% yield. Anal. Calcd for $C_{15}H_{24}IrN_7$: C, 36.42; H, 4.89; N, 19.82. Found: C, 36.40; H, 4.78; N, 20.00. ^1H NMR (200 MHz, $CdCl_3$): δ 1.824 (s, C_5Me_5, 15 H), 1.631 (s, *t*-BuNC, 9 H,); IR in C_6H_6: ν(CN) = 2170 cm^{-1}.

$Cp^*Ir(Ox)P(Me)_3$. $Cp^*Ir(Cl)_2P(Me)_3$ (200 mg, 0.422 mmol) was dissolved in 10 mL of methanol and added to a solution of $K_2Ox\cdot H_2O$ (5 g) dissolved in 50 mL of water. The solution was stirred at 45 °C for 5 h during which time the solution changed from a bright orange color to a light yellow. The aqueous solution was extracted with CH_2Cl_2 (5 × 50 mL). The CH_2Cl_2 layers were combined, dried with $MgSO_4$ and filtered. The solvent was removed under reduced pressure to give 143 mg (69% yield) of microcrystalline, lemon yellow product. Anal. Calcd for $C_{15}H_{24}IrO_4P$: C, 36.65; H, 4.93. Found: C, 36.72; H, 4.72. ^1H NMR (200 MHz, $CDCl_3$): δ 1.678 (d, C_5Me_5, 15 H, J_{P-H} = 2 Hz), 1.478 (d, $P(Me)_3$, 9 H, J_{P-H} = 10.6 Hz).

$Cp^*Ir(Ox)P(Cy)_3$. $Cp^*Ir(Cl)_2P(Cy)_3$ (338 mg, 0.221 mmol) and $K_2Ox\cdot H_2O$ (5 g) were added to 20 mL of methanol and stirred for 14 h. The methanol was then removed under reduced pressure, leaving a light yellow oil, which was dissolved in the minimum amount of CH_2Cl_2. Addition of hexane precipitated a lemon yellow microcrystalline product (220 mg, 93% yield). Anal. Calcd for $C_{30}H_{48}IrO_4P$: C, 51.78; H, 6.95. Found: C, 51.69; H, 7.08. ^1H NMR (200 MHz, $CDCl_3$): δ 1.678 (d, C_5Me_5, 15 H, J_{P-H} = 2 Hz), 1.478 (d, $P(Me)_3$, 9 H, J_{P-H} = 10.6 Hz).

$Cp^*Ir(Cl)_2P(Cy)_3$. $P(Cy)_3$ (70.7 mg, 0.252 mmol) was added to a solution of $[Cp^*Ir(Cl)_2]_2$ (100 mg, 0.126 mmol) in 15 mL of CH_2Cl_2, and an immediate color change from red to orange occurred. The solution was stirred for 3 h, the volume was reduced to ca. 5 mL, and hexane was added to precipitate a light orange microcrystalline product (126 mg, 74% yield). ^1H NMR (200 MHz, $CDCl_3$): δ 1.569 (d, C_5Me_5, 15 H, J_{P-H} = 1.6 Hz), 1.2–2.6 (m, $P(Cy)_3$, 33 H,).

NMR Photolysis Experiments. An illustrative example of a typical NMR-scale photolysis experiment is provided by the photolysis of $Cp^*Ir(N_3)_2P(Me)_3$ in C_6H_6. An NMR tube with about 5 mg of complex was attached to a vacuum line with an Ace NMR tube tip-off manifold. Degassed benzene dried over 4-Å sieves was distilled into the tube. After the sample was photolyzed for 4 h, the apparatus was reattached to the vacuum line and the C_6H_6 was removed and replaced with C_6D_6. The tube was then sealed, and ^1H NMR spectra were obtained.

Quantum Yield Determinations. Monochromatic light (313 or 365 nm) was obtained by filtering the output of a 100-W mercury vapor lamp with the appropriate interference filter (Oriel). The commercially available compound Aberchrome 540[19] was used as the actinometer. A solution of the actinometer in toluene was photolyzed at the appropriate wavelength and the appearance of the product was monitored at 494 nm. The resulting measurements showed that the lamp was very stable and provided highly reproducible light intensities. Typically, the flux at 313 nm was 7.1×10^{-8} einstein/min. Samples were prepared in an inert-atmosphere box with freeze–pump–thaw degassed solvents dried over molecular sieves. All solutions were stirred during photolysis. Quantum yields were determined by measuring the disappearance of either the azide or oxalate infrared stretch during the photolysis of approximately 2 mM solutions of complex. This concentration was sufficient to ensure complete absorption of the incident light. The data used for the quantum yield determinations were acquired for less than 10% conversion of starting material.

Results and Discussion

Photochemical Reactions. All of the new oxalate and bis(azide) compounds we report here are easily synthesized in high yields and are air-stable in the absence of ultraviolet light. Upon photolysis of these complexes, we have qualitatively observed the generation of CO_2 and N_2, respectively.[20] Two oxidative-addition reaction modes are observed under photolytic conditions: intramolecular reactions with coordinated L and/or intermolecular reactions with solvent. In general, either reaction mode is available from a given compound depending on the choice of solvent and the nature of L.

To gain some insight into the scope of the reaction chemistry available in these new systems, we have studied reactions in hydrocarbon and chlorinated solvents. Significant reactivity is indicated by the relatively high quantum efficiencies (vide infra) we measure for both the azide and oxalate complexes upon photolysis. In several cases, the reactions we observe parallel the observed reactivity of $Cp^*IrP(Me)_3(H)_2$ described by Bergman et al. For instance, consider the photochemical reaction of $Cp^*Ir(N_3)_2P(Me)_3$ with degassed benzene. The product exhibits a ^1H NMR resonance at −17.13 ppm (d, J_{P-H} = 36.7 Hz), con-

(12) (a) Paonessa, R. S.; Trogler, W. C. *Organometallics* **1982**, *1*, 768. (b) Paonessa, R. S.; Prignano, A. L.; Trogler, W. C. *Organometallics* **1985**, *4*, 647.
(13) Blake, D. M.; Nyman, C. J. *J. Am. Chem. Soc.* **1970**, *92*, 5329.
(14) Vaudo, A. F.; Kantrowitz, E. R.; Hoffman, M. Z.; Papaconstantinou, E.; Endicott, J. F. *J. Am. Chem. Soc.* **1972**, *94*, 6655.
(15) Endicott, J. F.; Hoffman, M. Z.; Beres, L. S. *J. Phys. Chem.* **1970**, *74*, 1021.
(16) Vogler, A.; Hlavatsch, J. *Angew. Chem., Int. Ed. Engl.* **1983**, *22*, 154.
(17) Booth, B. H.; Haszeldine, R. N.; Hill, M. *J. Chem. Soc.* **1969**, 1302.
(18) Rigby, W.; Bailey, P. M.; McCleverty, J. A.; Maitlis, P. M. *J. Chem. Soc. Dalton Trans.* **1979**, 371.
(19) Heller, H. G.; Langan, J. R. *J. Chem. Soc. Perkin Trans. 1* **1981**, 341.
(20) During the photolysis of $Cp^*Ir(Ox)(P(Me)_3)$ in $CHCl_3$ the appearance of a peak at 2337 cm^{-1} attributable to CO_2 was observed in the IR spectrum. An identical peak was generated by dissolving CO_2 in $CHCl_3$. Dinitrogen was identified as the major product gas in the photochemical reactions of the azide complexes by mass spectrometry.

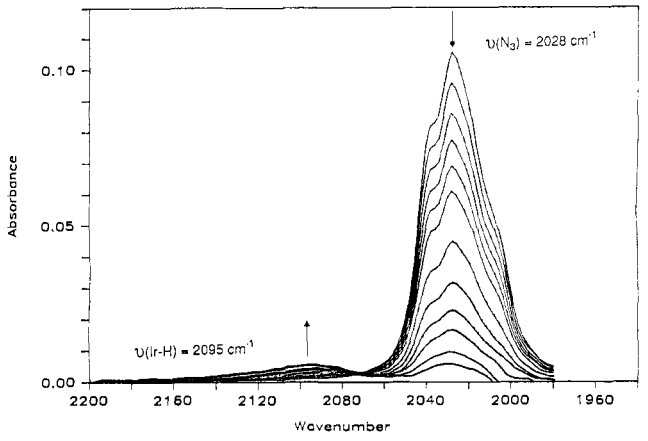

Figure 1. Infrared spectral changes that occur during the photolysis of a 0.0021 M solution of $Cp^*Ir(P(Me)_3(N_3)_2$ in benzene. Arrows indicate the direction of the absorbance changes with time. Spectra were taken at approximately 5 min intervals.

sistent with reported values for $Cp^*Ir(H)(Bz)(P(Me)_3)$. The reaction was also followed by infrared spectroscopy (Figure 1). Smooth, isosbestic conversion of the azide starting material ($\nu(N_3)$ = 2030 cm^{-1}) to the phenyl hydride is indicated by the growth of a weak metal–hydride stretch at 2100 cm^{-1}. When the same reaction is carried out in benzene-d_6, no hydride resonances are observed in the ^1H NMR spectrum and the peak at 2100 cm^{-1} is absent.[21] An analogous reaction of the oxalate complex also results in the formation of the hydride, but a significant amount of a second unidentified product is also formed. The relatively low solubility of the oxalate complex in benzene was a hindrance, and the further study of the reaction chemistry of the trimethylphosphine complex in this solvent was suspended. The more soluble triphenylphosphine complex, $Cp^*Ir(N_3)_2P(Ph)_3$, undergoes photolysis in benzene to produce a mixture of $Cp^*IrP(Ph)_3(H)(Ph)$ and the orthometalated product $Cp^*Ir(\mu\text{-}Ph)P(Ph)_2(H)$ in a 0.45/0.55 mole ratio that is identical within experimental error with the ratio reported by Bergman for the analogous dihydride. This latter result strongly suggests that an intermediate similar to the one generated from the dihydride complex is also generated from the bis(azide).

As previous workers have observed,[2,22] we suggest that steric effects at the metal in the photogenerated intermediate are also important in determining the ultimate course of the oxidative addition. Irradiation of both azide and oxalate complexes with L = tricyclohexylphosphine produce exclusively orthometalated products. The photolysis of either tricyclohexylphosphine complex initially produces one set of hydride peaks centered at −16.30 ppm (J_{P-H} = 28.2Hz), and later, after virtually all the starting material is consumed, a new hydride doublet appears at −16.69 ppm (J_{P-H} = 28Hz) at the expense of the original doublet. After the two sets of peaks reach approximately equal intensities, continued photolysis causes both sets of hydride peaks to disappear. We believe that the two products arise from attack by the metal at either the axial or equatorial hydrogen on the a carbon of the cyclohexyl ring. The data suggest that one isomer forms preferentially in the initial photolysis but is then partially converted to the other isomer by continued photolysis. The ^{13}C NMR spectrum of approximately a 1:1 mixture of the two forms is shown in Figure 2. The resonances from the ring and methyl carbons (a and b), of the Cp* ligand are almost unchanged from the starting material. We confirmed the assignment of carbon c by a ^{13}C DEPT NMR study that indicates that the resonance assigned to carbon c has a multiplicity of 1. This result eliminates all the cyclohexyl ring carbons with the exception of the metal- and phosphine-bound carbons. Further, the large ^{13}C-^{31}P coupling constants (J_{C-P} = 30.4 Hz for the downfield peak and 35.0 Hz for the upfield peak) are only consistent with assignment as the phosphine-bound carbon. The peaks assigned as the metal-bound ring carbons were also shown by the DEPT study to have a multiplicity of 1, and the upfield shift is similar to the position reported for the carbon bound to the iridium in $Cp^*IrP(Me)_3(Cy)H$.[2] The similar reactivity of $Cp^*Ir(P(Cy)_3)Ox$ and $Cp^*Ir(P(Cy)_3)(N_3)_2$ with respect to reaction with C–H bonds suggests that common intermediates (probably $Cp^*Ir(P(Cy)_3)$) are formed from both precursors.

Scheme I

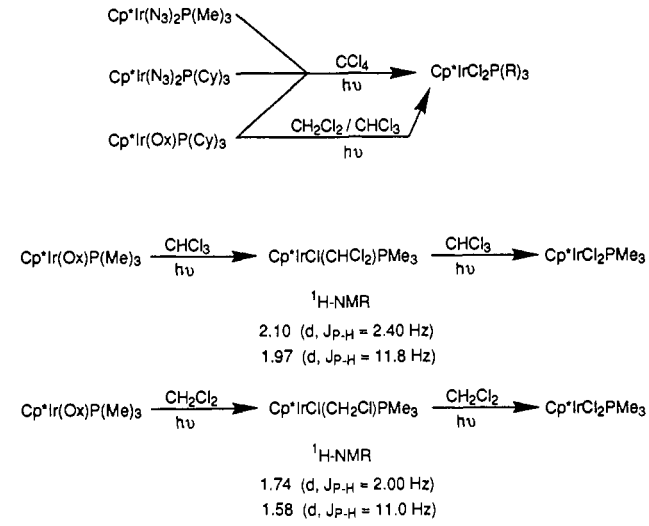

As expected for systems capable of reaction with C–H bonds, the photoreactions of these oxalate and bis(azide) complexes with halocarbons are also quite facile, and illustrate an interesting pattern of reactivity. As shown in Scheme I, the final product observed during photolysis in chlorinated solvents is generally the corresponding dichloride. In the reactions with halocarbons of decreased reactivity, intermediate species can be detected. During the photolysis of $Cp^*Ir(Ox)P(Me)_3$ in $CHCl_3$ or CH_2Cl_2, the growth and subsequent decay of similar intermediate species are detected by ^1H NMR spectroscopy. The intermediate is formed in much greater concentrations in the CH_2Cl_2 case than it is for $CHCl_3$. We propose that in both cases the intermediates are complexes formed from initial oxidative addition of a solvent C–Cl bond to form $Cp^*Ir(CHCl_2)Cl(P(Me)_3)$ (product in $CHCl_3$) or $Cp^*Ir(CH_2Cl)Cl(P(Me)_3)$ (product in CH_2Cl_2). These complexes then react further to produce the dichloride and undetermined organic products. The ^1H NMR data for the two intermediates are shown in Scheme I. As the carbon-bound moiety formed on oxidative addition of the C–Cl bond becomes more electron withdrawing due to the exchange of a hydrogen for a chlorine, the two resonances show the expected downfield shift. Similar reactivity is observed in previously studied platinum–oxalate chemistry. For example, Trogler notes that photolysis of $Pt(PEt_3)_2(C_2O_4)$ in the presence of CH_3Cl produces the stable complex $Pt(PEt_3)_2(CH_3)(Cl)$[12] while Blake reports that $Pt[P(C_6H_5)_3]_2C_2O_4$[13] reacts with $CHCl_3$ to produce the dichloride. In this latter case, no intermediates were observed.

We were also interested in investigating the relative intramolecular reactivity of C–H bonds versus intermolecular C–Cl bonds. We addressed this point by determining that photolysis of $Cp^*Ir(Ox)PCy_3$ in $CHCl_3$ and CH_2Cl_2 produces exclusively the dichloride. As in the case of the $P(Me)_3$ complex, the presence of an intermediate was detected in the ^1H NMR spectrum of the reaction in CH_2Cl_2. An intermediate was not detected in the reaction with $CHCl_3$, perhaps because of interferences by overlapping $P(Cy)_3$ resonances. Somewhat surprisingly, none of the azide complexes react with either $CHCl_3$ or CH_2Cl_2 to produce readily identifiable products;[14] however, both $Cp^*Ir(N_3)_2P(Me)_3$ and $Cp^*Ir(N_3)_2P(Cy)_3$ react with CCl_4 to generate the corresponding dichloride, but the $P(Me)_3$ complex also produces some byproducts. The differences in reactivity exhibited by the azide and oxalate complexes toward CH_2Cl_2 and $CHCl_3$ suggest either

(21) The region where the Ir–D stretch should appear is obscured by solvent peaks.
(22) Crabtree, R. H. *Chem. Rev.* **1985**, *85*, 245.

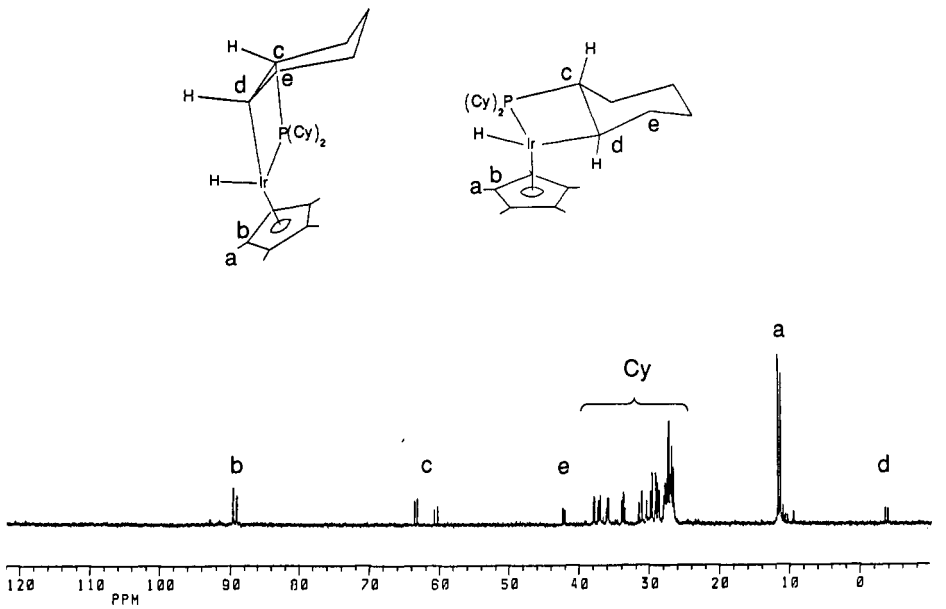

Figure 2. ^{13}C NMR spectrum of the products generated upon photolysis of $Cp^*Ir(P(Cy)_3)(Ox)$ in benzene.

that the reaction intermediates are not common to both the azide and oxalate systems or the initial hydrido oxidative-addition products undergo secondary reactions with azide but not with oxalate.

Quantum Yields. Only a small amount of quantitative information is available with regard to the quantum yields that characterize reactions 1[23] and 2. This is understandable given the highly air-sensitive nature of the dihydride and bis(carbonyl) precursors. Because we have observed strikingly similar chemistry, and the precursors are easily handled, we have measured quantum yields for several of the photochemical reactions discussed previously in this paper. Our measurements are presented in Table I.

We observe little variation in the disappearance quantum yields for the photolysis of the three azide complexes in benzene solutions (ϕ = 0.067, 0.045, and 0.073, for L = PMe_3, PCy_3, and *t*-BuNC). This result is somewhat surprising because the reaction products vary considerably from inter- to intramolecular C–H bond activation. Additionally, the quantum yield values for reactions of $Cp^*Ir(P(Cy)_3)(N_3)_2$ and $Cp^*Ir(P(Me)_3(N_3)_2$ in $CHCl_3$ (ϕ = 0.032, 0.067) and CH_2Cl_2 (ϕ = 0.029, 0.063) differ only slightly from the values for reactions in benzene. The independence of ϕ with respect to the identity of L and substrate suggests several points. First, the reactivity of these azide complexes is only weakly dependent on changes in the electron density at the metal for the complexes we studied. We expected that the variation of L from $P(Mc)_3$ to $P(Cy)_3$ to *t*-BuNC would result in significant changes in reactivity. We also suggest that, within the range of compounds studied, the reactive intermediate is generated with similar efficiency regardless of the electronic environment about the metal. Additionally, the similarity in ϕ for photolysis in solvents with widely differing reactivities indicates that the net reaction efficiencies are not determined by the rates of reaction of the photogenerated intermediates but are more likely determined by photophysical factors (i.e., similar nonradiative decay rates of the excited-state precursors). In contrast to the data gathered for the azide complex reactions in $CHCl_3$ and CH_2Cl_2, the quantum yields for reactions of both the $P(Me)_3$ and $P(Cy)_3$ azide complexes in CCl_4 are significantly greater than for reactions in benzene and suggest that the reactions in CCl_4 may be mechanistically different from the other photoreactions (vide infra).

We also collected quantum yields for the reactions of the oxalate complexes in several solvents. Surprisingly, the observed quantum yield values for the oxalates in $CHCl_3$ and CH_2Cl_2 are significantly *less* than those for C–H bond activation in the orthometalation reaction. This result is contrary to previously observed relative reactivities of C–H and C–Cl bonds. We attribute the observed decrease in these quantum yields to increases in the nonreactive, nonemissive deactivation of the excited state caused by differences in solvent–complex interactions. In studies of $Pt(C_2O_4)(PEt_3)_2$,[24] Trogler and co-workers noted that the quantum yield for photolysis in acetonitrile was inversely dependent on the concentration of water present in the solution. They attributed this to hydrogen bonding of water molecules to the oxalate carbonyl oxygens, which provides an efficient path for deactivation of the excited state via energy transfer to solvent. Additional evidence for the H-bonding interaction was provided by changes in intensity and position of the oxalate bands in the presence of water. Gray et al.[25] have also observed a large diminution of the emission quantum yield and lifetime of $ReO_2(py)_4^+$ in the presence of hydrogen bond donors such as water. Our observations are novel in that they suggest $CHCl_3$ and CH_2Cl_2 also hydrogen bond to the coordinated oxalate group of $Cp^*Ir(Ox)(L)$ complexes. In support of this hypothesis, we offer the IR spectra (Figure 3) of $Cp^*Ir(Ox)P(Cy)_3$ obtained in three different solvents. Clearly discernible differences

Table I. Quantum Yields for Iridium(III) Azide and Oxalate Complexes

complex	solvent	ϕ
$Cp^*Ir(N_3)_2P(Me)_3$	benzene	0.067
$Cp^*Ir(N_3)_2P(Me)_3$	benzene	0.052[b]
$Cp^*Ir(N_3)_2P(Me)_3$	$CHCl_3$	0.067
$Cp^*Ir(N_3)_2P(Me)_3$	CH_2Cl_2	0.063
$Cp^*Ir(N_3)_2P(Me)_3$	CCl_4[c]	0.28
$Cp^*Ir(N_3)_2P(Cy)_3$	benzene	0.045
$Cp^*Ir(N_3)_2P(Cy)_3$	CCl_4	0.27
$Cp^*Ir(N_3)_2P(Cy)_3$	$CHCl_3$	0.032
$Cp^*Ir(N_3)_2P(Cy)_3$	CH_2Cl_2	0.029
$Cp^*Ir(N_3)_2$-*t*-BuNC	benzene	0.073
$Cp^*Ir(Ox)P(Cy)_3$	benzene	0.089
$Cp^*Ir(Ox)P(Cy)_3$	benzene[d]	0.098
$Cp^*Ir(Ox)P(Cy)_3$	CCl_4/benzene[c]	0.16
$Cp^*Ir(Ox)P(Cy)_3$	$CHCl_3$	0.022
$Cp^*Ir(Ox)P(Cy)_3$	CH_2Cl_2	0.017
$Cp^*Ir(Ox)P(Me)_3$	$CHCl_3$	0.020
$Cp^*Ir(Ox)P(Me)_3$	CH_3OH	0.0064

[a] All values reported for irradiation at 313 nm unless otherwise noted. Quantum yields are ±10%. [b] Irradiated at 365 nm. [c] Sample was irradiated in a 3:1 mixture of CCl_4/benzene. [d] Irradiated under approx. 1 atm CO_2.

(23) Marx, D. E.; Lees, A. J. *Inorg. Chem.* **1988**, *27*, 1121.

(24) Prignano, A. L.; Trogler, W. C. *Inorg. Chem.* **1986**, *25*, 4454.
(25) Winkler, J. R.; Gray, H. B. *Inorg. Chem.* **1985**, *24*, 346.

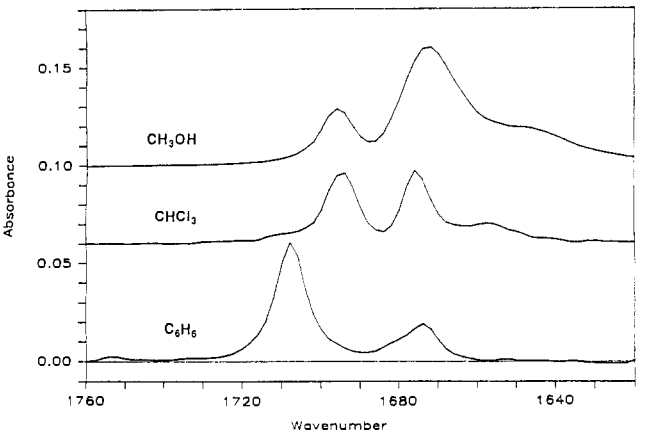

Figure 3. Infrared spectra of $Cp^*Ir(P(Cy)_3)(Ox)$ in CH_3OH, $CHCl_3$ and C_6H_6.

Scheme II. Proposed Photochemical Reaction Scheme

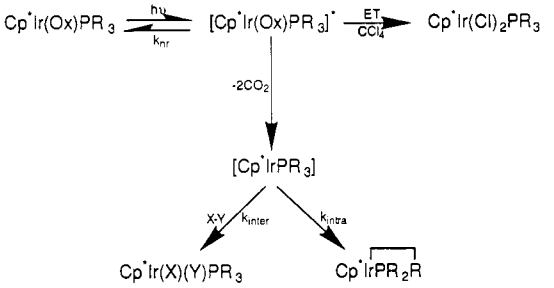

in the oxalate bands occur when the solvent is changed from a non-hydrogen-bonding solvent (benzene) to a weakly hydrogen-bonding solvent ($CHCl_3$) to a strong hydrogen-bonding solvent (MeOH). Additional support that H bonding between coordinated oxalate and the solvent is very significant and lowers the reaction quantum yield comes from the surprising result that the *apparently* highly hydrophobic $Cp^*Ir(P(Me)_3)Ox$ complex is freely soluble in water and is very stable to prolonged photolysis in this solvent.[26]

As for the azide complexes, the quantum yield for reaction of $Cp^*Ir(Ox)(P(Cy)_3)$ in CCl_4 is significantly greater than that in benzene or in the other chlorinated solvents. We suggest that for both the azide and oxalate compounds this enhanced reactivity is due to significant mechanistic differences for the CCl_4 reactions. We suggest that the CCl_4 reactions might entail direct electron transfer from the photogenerated excited state to the solvent. Further work will obviously be needed to substantiate or refute this suggestion.

Our conclusions concerning the sequence of photochemically induced events for these complexes are summarized in Scheme II, which is illustrated for the oxalate compounds. We believe that excitation of any of the oxalate complexes produces a putative excited state that can either nonradiatively decay back to the ground state (rate constant k_{nr}), lose two molecules of CO_2 in a mechanistically undetermined sequence of steps to yield a $16e^-$, coordinatively unsaturated complex (Cp^*IrL), or, in the case of CCl_4, undergo electron transfer to the solvent. The loss of CO_2 (or N_2 in the case of the azide complexes) is irreversible as judged by the lack of an inhibition effect on the quantum yield in the presence of CO_2 or N_2. The variations in the quantum yields we have observed for the oxalate compounds with H-bonding ability of the solvent and the lack of variation for the azide compounds suggest these reaction quantum yields are controlled almost entirely by variations in k_{nr}. With the oxalate complexes, changes in k_{nr} lead to large changes in ϕ because k_{nr} is readily enhanced by hydrogen bonding between the complex and solvent. This effect is apparently absent with the azide complexes and leads to smaller variations in the quantum yield. Consistent with these ideas, none of the azide complexes show any significant solvent effects (shifts in intensity or energy) on the azide IR stretching bands.

Conclusions

We have synthesized several new oxalate and bis(azide) complexes of the form $Cp^*Ir(Ox)L$ and $Cp^*(N_3)_2L$. Upon photolysis, these complexes undergo reactions that result in the elimination of CO_2 or N_2 to give reactive intermediates that undergo oxidative-addition reactions with C–H and C–Cl bonds. The reactions result in either inter- or intramolecular oxidative addition of C–H or C–Cl bonds to the Ir center. The quantum yields for these reactions are in the range 0.01–0.3 and are controlled by the nonradiative decay rate of the excited state. The magnitude of the quantum yield appears to correlate inversely with the hydrogen-bonding ability of the solvent in the case of the oxalate complexes but not in the case of the bis(azide) complexes. IR spectral data indicate significant shifts for the $\nu(CO)$ frequencies of the oxalate bands in solvents of even moderate H-bonding ability.

Acknowledgment. We thank Johnson Matthey for the generous loan of iridium trichloride. D.A.F. acknowledges support from the University of Minnesota Graduate School. This material is based upon work supported in part by the National Science Foundation under Grant No. CHE-8722843. The U.S. Government has certain rights in this material.

(26) The ^{13}C NMR spectrum of $Cp^*Ir(P(Me)_3)Ox$ in aqueous solution exhibits a sharp singlet at 169.35 ppm for the coordinated oxalate carbons. Addition of K_2Ox to this solution leaves the coordinated oxalate signal unchanged and results in an additional resonance due to free oxalate at 176.23 ppm.